MCB
Journals.ASM.org

Mex3c Mutation Reduces Adiposity and Increases Energy Expenditure

Yan Jiao,[a] Sunil K. George,[a] Qingguo Zhao,[a] Matthew W. Hulver,[b] Susan M. Hutson,[b] Colin E. Bishop,[a] and Baisong Lu[a]

Institute for Regenerative Medicine, Wake Forest University Health Sciences, Winston-Salem, North Carolina, USA,[a] and Department of Human Nutrition, Foods, and Exercise, Virginia Polytechnic Institute and State University, Blacksburg, Virginia, USA[b]

The function of MEX3C, the mammalian homolog of *Caenorhabditis elegans* RNA-binding protein muscle excess 3 (MEX-3), was unknown until our recent report that MEX3C is necessary for normal postnatal growth and enhances the expression of local bone *Igf1* expression. Here we report the pivotal role of *Mex3c* in energy balance regulation. *Mex3c* mutation caused leanness in both heterozygous and homozygous transgenic mice, as well as a more beneficial blood glucose and lipid profile in homozygous transgenic mice, in both sexes. Although transgenic mice showed normal food intake and fecal lipid excretion, they had increased energy expenditure independent of physical activity. Mutant mice had normal body temperature, *Ucp1* expression in brown adipose tissue, and muscle and liver fatty acid oxidation. *Mex3c* is expressed in neurons and is detectable in the arcuate nucleus, the ventromedial nucleus, and the dorsomedial nucleus of the hypothalamus. *Mex3c* was not detected in NPY or POMC neurons but was detected in leptin-responsive neurons in the ventromedial nucleus. *Mex3c* and *Leptin* double mutant mice were growth retarded and obese and had blood profiles similar to those of *ob/ob* mice but showed none of the steatosis observed in *ob/ob* mice. Our data show that *Mex3c* is involved in energy balance regulation.

Caenorhabditis elegans MEX-3 is an hnRNP K homology (KH) domain-containing RNA-binding protein regulating RNA targets such as *pal-1* (13, 22, 23), *rme-2* (6), and *nos-2* (25). It is involved in the cell fate specification process in *C. elegans* and in totipotency maintenance of the germ line in adult worms (7, 13, 23, 40). Human and mouse genomes encode four MEX-3 homologues: MEX3A, MEX3B, MEX3C, and MEX3D (3). They all have two KH RNA-binding domains at the N terminus which are also present in the *C. elegans* homolog and a zinc finger (ZNF) domain at the C terminus which is absent in MEX-3 in *C. elegans*. MEX3A and MEX3B colocalize with decapping factor DCP1a and Argonaute proteins in processing bodies (3), and the localization of MEX3B is regulated by 14-3-3 protein (9). MEX3D, once called TINO, is a *BCL2* mRNA AU-rich element-binding protein that negatively regulates the stability of *BCL2* mRNA (12).

Mouse MEX3C is 99% identical to human, chimpanzee, and bovine MEX3Cs. Linkage analysis and association studies suggest that *MEX3C* contributes to genetic susceptibility of hypertension (21), although the mechanism is unknown. Recently, we reported that *Mex3c* mutation in mice causes growth retardation due to IGF1 deficiency in developing bone (26). *Mex3c* is highly expressed in resting and proliferating chondrocytes, and IGF1 protein expression in these cells of mutant mice is significantly reduced, although *Igf1* mRNA expression in bones from mutant mice is not changed. In the C57BL/6 background, 85% of homozygous mutant pups die soon after birth, whereas in the FVB/N background, about 80% of the pups survive to adulthood, although they are still growth retarded. Mutant male and female mice are fertile, although *Mex3c* is highly expressed in the testis and ovary. *Mex3c* is also highly expressed in the brain, but its function in the nervous system is unknown.

While examining the postnatal growth of *Mex3c* gene trap mice, we observed that in addition to growth retardation, homozygous mutant mice have reduced adiposity compared to age-matched control mice. *Mex3c* expression is low in the liver, muscle, and adipose tissues but high in the brain. The hypothalamus of the brain plays a major role in the control of energy balance (35). Nuclei in the hypothalamus, such as the arcuate nucleus (ARC), the ventromedial nucleus (VMN), and the dorsomedial nucleus (DMN), contain multiple neurons that receive signals from insulin and leptin and project to the other regions of the brain to regulate food intake and energy expenditure (10, 11, 15). In the ARC, neuropeptide Y (NPY) and Agouti-related peptide (AgRP), coexpressed by NPY neurons, stimulate food intake and inhibit energy expenditure (2, 5, 14, 36, 48). Gene products from proopiomelanocortin (POMC) and cocaine- and amphetamine-regulated transcript (CART) coexpressed by POMC neurons suppress food intake and promote energy expenditure (29, 43). α-Melanocyte-stimulating hormone (αMSH), a peptide from proopiomelanocortin, is an agonist of the melanocortin-4 receptor (MC4R) (18, 24, 38), while AgRP is an antagonist of MC4R (32). Steroidogenic factor 1 (SF-1)-positive neurons in the hypothalamic VMN are also important in controlling energy balance. SF-1 knockout mice have abnormal VMN and become obese, mostly from decreased activity rather than increased food intake (11, 34).

The observations of the lean phenotype of *Mex3c* mutant mice and the high level of *Mex3c* expression in the brain prompted us to examine the possible role of *Mex3c* in energy balance regulation. Here we report that *Mex3c* mutation reduces adipose deposition and increases energy expenditure in both heterozygous and homozygous mutant mice. We propose that *Mex3c* could be involved in central energy balance regulation.

MATERIALS AND METHODS

Animals. *Mex3c* gene trap mice were described recently (26). Mice were initially of mainly the C57BL/6 background, but after showing a high rate of perinatal lethality in this background, they were backcrossed to the

Received 5 April 2012 Returned for modification 27 April 2012
Accepted 14 August 2012
Published ahead of print 27 August 2012
Address correspondence to Baisong Lu, blu@wakehealth.edu.

doi:10.1128/MCB.00452-12

FVB/N background for 4 generations. Heterozygous +/*tr* ("*tr*" indicates the trapped allele) breeding pairs were used to obtain +/+, +/*tr*, and *tr/tr* mice for the study. *Lep*$^{ob/ob}$ mice (49), *Npy*-GFP mice (which specifically express green fluorescent protein [GFP] in NPY/AgRP neurons) (44), and *Pomc*-GFP mice (which specifically express GFP in POMC neurons) (10) were purchased from the Jackson Laboratory. Double-positive transgenic mice were obtained by crossing *Mex3c*$^{+/tr}$ females (mainly of the FVB/N background) with the other transgenic males. *Mex3c*; *ob/ob* double mutant mice were of a mixed C57BL/6 and FVB/N background. Doubly heterozygous breeding pairs were used to generate double mutant mice. Genotyping for *Mex3c* mutant mice was performed as described previously (1, 26). GFP-positive mice were identified by positive PCR amplification of a product with the primers *GFPF* (ACGTAAACGGCCACAAG TTC) and *GFPR* (AAGTCGTGCTGCTTCATGG). Genotyping for the *Lep*^{ob} allele was performed according to the protocol recommended by the Jackson Laboratory.

Mice were housed in the animal facility of Wake Forest University Health Sciences. Experiments were conducted in accordance with the *Guide for the Care and Use of Laboratory Animals* (40a) and approved by the Institutional Animal Care and Use Committee of Wake Forest University Health Sciences. Mice were kept in microisolator cages with 12-h light-dark cycles and were fed *ad libitum*. Mice were fed a chow diet (Prolab; PMI Nutrition International, Henderson, CO) during all experiments.

Glucose and insulin tolerance tests. For glucose tolerance tests, mice were fasted overnight for 16 h. Just before glucose injection, tail vein blood glucose was measured with an Accu-Chek active meter and test strips (Roche) to obtain a reading for time zero. The mice then received an intraperitoneal injection of sterile 10% D-glucose (Sigma) at a dosage of 1 g/kg body weight. Blood glucose levels were measured 30, 60, 90, and 120 min after glucose injection.

For insulin tolerance tests, mice were fasted for 6 h. Just before insulin injection, tail vein blood glucose was measured with an Accu-Chek active meter and test strips (Roche) to obtain a reading for time zero. The mice then received an intraperitoneal injection of 0.75 U/kg insulin (Novo Nordisk) prediluted to 2.5 U/ml in 0.9% NaCl. Blood glucose levels were measured 30, 60, 90, and 120 min after insulin injection.

For both assays, each group contained 5 or more animals. Data were analyzed by analysis of variance (ANOVA).

MRI to determine fat composition. The fat composition of *Mex3c* mutant mice was determined without anesthesia, using a Bruker LF90 TD system (Bruker Optics) operated by Virginia Polytechnic Institute and State University. The fat composition of *Mex3c* and *Leptin* double mutant mice was determined with a Bruker Biospin 7T micro-magnetic resonance imaging (micro-MRI) scanner (Center for Biomolecular Imaging, Wake Forest University Health Sciences) after mice were anesthetized with 1.5% to 2% isoflurane. Images were analyzed using ImageJ software to measure the total fat volume in each mouse. A density of 0.92 g/ml was used to calculate the weight of adipose tissue (27).

Blood biochemical assays. Plasma was collected from mice fasted for 6 h. Blood triglyceride and cholesterol concentrations were assayed with kits from Cayman Chemical (Ann Arbor, MI). Insulin and leptin concentrations were assayed with enzyme-linked immunosorbent assay (ELISA) kits from Mercodia (Uppsala, Sweden) and Millipore (Billerica, MA), respectively. All assays were performed according to the manufacturer's instructions.

Body temperature. Core body temperature was monitored by measuring the rectal temperature of conscious mice. Each mouse was assayed at noon on two successive days, and the average was obtained for analysis. A Thermalert model TH-5 temperature monitor (Physitemp, Clifton, NJ) was used, with the probe placed in the rectum to a depth of 1 cm.

Food consumption. For determination of food intakes of 6- and 10-week-old *tr/tr* mice, 2 or 3 mice were caged together during the assay, since *tr/tr* mice quickly lost significant body weight when caged singly. Normal control (+/+) mice and heterozygous mutant (+/*tr*) mice were singly caged in cages with lifted-wire bottoms and were allowed to adapt to the environment for at least 1 week before food consumption was examined. Food intake was monitored daily for 6 to 7 days, and the average for each mouse was used for analysis. Food spilled on the bottom of the cages was recovered and subtracted from food intake, which was then normalized to lean mass if animals showed differences in fat composition.

TABLE 1 Primers used for real-time PCR

Gene	Forward primer	Reverse primer
Npy	TACTACTCCGCTCTGCGACA	GATGAGGGTGGAAACTTGGA
Agrp	TGTGTTCTGCTGTTGGCACT	GACTCGTGCAGCCTTACACA
Pomc	GTCCCTCCAATCTTGTTTGC	TTTTCAGTCAGGGGCTGTTC
Cartpt	GCCCTGGACATCTACTCTGC	GTCGTCCCTTCACAAGCACT
Pparγ	TCTTAACTGCCGGATCCACAA	GCCCAAACCTGATGGCATT
Pgc1α	CCCTGCCATTGTTAAGACC	TGCTGCTGTTCCTGTTTTC
Ucp2	GAGAGTCAAGGGCTAGTGC	GCTTCGACAGTGCTCTGGTA
Mex3c	ATGCTGTCCCACGCCTAC	AGTGCTTTAATTTTACAACC CTGG
Socs3	GCCCCTTTGTAGACTTCACG	AACTTGCTGTGGGTGACCAT

Fecal lipid content. Feces were collected from mice in cages with lifted-wire bottoms. Fecal lipids were extracted as described by Folch et al. (16). Briefly, feces were collected from mice housed individually in cages with lifted-wire bottoms over a 24-h period. Five-hundred-milligram aliquots of feces were cleaned and dried for 1 h at 70°C, incubated with 2 ml of chloroform-methanol (2:1) for 30 min at 60°C with constant agitation, and then centrifuged. Water (1 ml) was added to the supernatant and then, following vortexing, phase separation was induced by low-speed centrifugation (2,000 rpm for 10 min). The lower, chloroform phase was then removed and transferred to a new tube, and the sample was evaporated to dryness. The mass of the total lipid (typically 15 to 20 mg) was obtained by subtracting the weight of the tube with lipid by the weight of the same tube without lipid, weighed with a balance reading to 0.1 mg.

Metabolic studies. Indirect calorimetry and locomotor activity measurements were performed using a Labmaster system (TSE Systems) at Virginia Polytechnic Institute and State University. Animals were tested at 12 weeks of age, before +/+ and +/*tr* mice showed obvious differences in body weight and fat composition. VO_2 consumption and VCO_2 production in individual mice were measured using metabolic chambers, and the respiratory exchange ratio (RER) was calculated to reflect energy expenditure. A photobeam-based activity monitoring system detected and recorded ambulatory movements. Energy expenditure (kJ/h) was calculated using the formula $VO_2 \times [3.815 + (1.232 \times RER)] \times 4.1868$ (45) and normalized to the lean mass determined by MRI. All parameters were measured continuously and simultaneously for 72 h after 36 h of adaptation for singly housed mice. Three-day averages for each mouse were used for analysis.

Assay of fatty acid and glucose oxidation. Red and white muscle tissues from quadriceps and gastrocnemius muscles were isolated for analysis. Fatty acid oxidation in whole-tissue homogenates was assessed by measuring and summing $^{14}CO_2$ production and ^{14}C-labeled acid-soluble metabolites from the oxidation of [1-^{14}C]palmitic acid (Perkin-Elmer, Waltham, MA), as previously described (17). Neutral lipids were extracted, and incorporation of [1-^{14}C]palmitic acid was measured using an AR 2000 TLC plate scanner (Bioscan, Washington, DC). Glucose oxidation in whole-muscle homogenates was assessed by measuring $^{14}CO_2$ production from the oxidation of [U-^{14}C]glucose (Perkin-Elmer, Waltham, MA).

Quantitative RT-PCR. RNA extraction, reverse transcription (RT), and quantitative PCR were performed as previously described (20, 26). TaqMan probes were used for mouse *Ucp1* and *Hprt1* (internal control) real-time PCRs. For real-time PCR analysis of the rest of the genes, primers used with SYBR green mixture are listed in Table 1. Results are presented as means ± standard errors of the means (SEM).

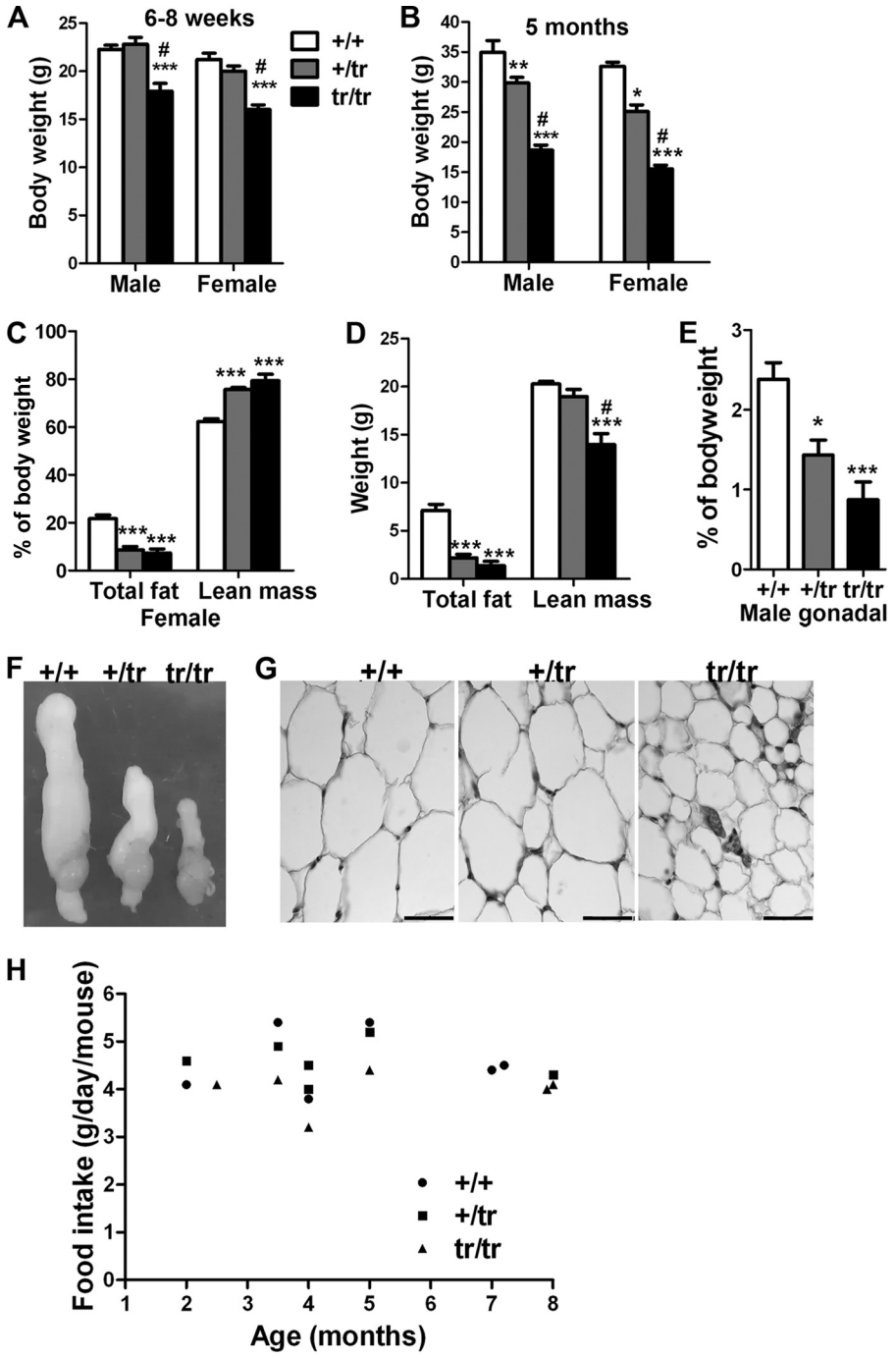

FIG 1 *Mex3c* mutation reduces adiposity. (A and B) Body weight of control and mutant mice at 6 to 8 weeks of age ($n \geq 6$/genotype) (A) and 5 months of age ($n = 6$/genotype for males and $n = 4$/genotype for females) (B). (C and D) Magnetic resonance imaging analysis of 5-month-old female mice from panel B. (E) Gonadal fat percentages of 5-month-old males. (F) Testes and gonadal fat pads of 5-month-old male mice. (G) Histological analysis of adipose tissue. Shown are gonadal fat sections from 7-month-old males. Adipocyte size was reduced in *tr/tr* mice, regardless of sex and age. (H) Food intake of male mice at different ages. For panels A to E, means and SEM are presented. *, **, and *** indicate P values of <0.05, <0.01, and <0.0001, respectively, compared with +/+ mice. #, $P < 0.0001$ compared with +/*tr* mice. Data were analyzed by Bonferroni posttests (A to D) or Tukey's multiple-comparison tests (E) following ANOVA.

X-Gal and immunostaining of brain cryosections. Brains from *Mex3c*$^{+/+}$, *Mex3c*$^{+/tr}$, *Npy-Gfp*; *Mex3c*$^{+/tr}$, and *Pomc-Gfp*; *Mex3c*$^{+/tr}$ mice were fixed with 4% paraformaldehyde (PFA) at 4°C for 2 h, immersed in 30% sucrose–phosphate-buffered saline (PBS) overnight at 4°C, and then embedded in OCT for cryosectioning. To examine *Mex3c* expression in leptin-responsive neurons, mice were fasted for 16 h and then injected intraperitoneally with 5 μg/g (body weight) mouse leptin (PeproTech, Rocky Hill, NJ). One hour later, the mice were perfused with PBS for 10 min followed by 4% PFA for 10 min, and the brains were recovered for cyrosectioning. The sections were processed as described previously before p-STAT3 antibody staining (39). X-Gal (5-bromo-4-chloro-3-indolyl-β-D-galactopyranoside) staining of mouse brain cryosections (to ex-

TABLE 2 Food intake of *Mex3c* mutant mice[a]

Age	Sex	Food intake parameter	Mean value ± SEM for group (no. of mice in group)		
			+/+	+/*tr*	*tr*/*tr*
6 wk	Male	g/day/mouse	5.1 ± 0.1 (10)	5.3 ± 0.2 (8)[b]	3.2 ± 0.18 (7)[d]
	Male	g/day/g body weight	0.23 ± 0.01	0.23 ± 0.01[b]	0.20 ± 0.04
10 wk	Female	g/day/mouse	4.7 ± 0.10 (6)	5.0 ± 0.15 (7)[b]	2.9 ± 0.17 (10)[d]
	Female	g/day/g body weight	0.23 ± 0.01	0.26 ± 0.01[c]	0.18 ± 0.01[d]
3 mo	Female	Daily food intake (g)	4.5 ± 0.24 (5)	ND	3.3 ± 0.17 (5)[d]
	Female	Food intake/lean mass	0.29 ± 0.03	ND	0.28 ± 0.01

[a] With the exception of 6- and 10-week-old *tr*/*tr* mice, which were group caged, all other mice were singly caged for food intake assays. Data were analyzed by Tukey's multiple-comparison test following ANOVA (for 6- and 10-week-old mice) or by *t* tests (for 3-month-old mice). *P* values of <0.05 were regarded as statistically significant. ND, data not determined.
[b] No significant difference compared with +/+ mice.
[c] Significantly higher than the value for +/+ mice.
[d] Significantly lower than the value for +/+ mice.

amine the expression of *Mex3c* by detecting β-galactosidase activity) was performed as described previously (26); in some cases, eosin counterstaining was performed for better views of β-galactosidase-negative areas. For immunostaining, cryosections were fixed with 4% PFA, blocked with Protein Block (Dako) for 1 h, and incubated with anti-β-galactosidase antibody (Abcam; 1:500), with or without anti-β-III tubulin antibody (Millipore; 1:1,000) or anti-p-STAT3 (Cell Signaling; 1:200) antibody, at 4°C overnight. After three 5-min washes in Tris-buffered saline with Tween 20 (TBST), the sections were incubated with Alexa Fluor 594-conjugated anti-rabbit secondary antibody or Alexa Fluor 594-conjugated anti-rabbit and fluorescein isothiocyanate (FITC)-conjugated anti-mouse secondary antibodies (Invitrogen; 1:300) at room temperature for 1 h. The sections were mounted in mount medium containing DAPI (4′,6-diamidino-2-phenylindole; Vector). Images were taken with an Axio M1 microscope equipped with an AxioCam MRc digital camera (Carl Zeiss) or with an Eclipse TE2000-U confocal microscope (Nikon).

MEF cell isolation and *in vitro* adipocyte differentiation. Mouse embryonic fibroblast (MEF) cells were isolated from 12.5-day-old embryos after removing the brain and dark red organs. The embryonic tissues were finely minced with razor blades, treated with 2 ml/embryo 0.05% trypsin-EDTA, and incubated with gentle shaking at 37°C for 15 min. Cell suspension free of tissues was spun down in growth medium (minimum essential medium alpha [MEM-α] with 10% fetal bovine serum [FBS] and antibiotics) and plated in tissue culture dishes for growth. Passage 0 or passage 1 mouse embryonic fibroblast cells were induced for adipogenic differentiation as described previously (19). Cells were stained for lipid vacuoles by Oil Red O 2 weeks after induction. Oil Red O staining of differentiated adipocytes and liver cryosections was performed as described previously (31).

RESULTS

***Mex3c* mutation causes leanness in mice.** Although heterozygous *Mex3c* gene trap mice (+/*tr*) had body weights similar to those of +/+ mice at 6 to 8 weeks of age (Fig. 1A), they weighed significantly less than +/+ mice at 5 months (Fig. 1B). This was due mainly to reduced body fat deposition. Magnetic resonance imaging analysis of 5-month-old female mice found significantly reduced total fat mass and increased lean mass percentages in +/*tr* and *tr*/*tr* mice compared with +/+ mice (Fig. 1C). Reduced body weight in +/*tr* mice was fully accounted for by reduced fat deposition, since their lean mass did not differ from that of +/+ mice (Fig. 1D). Adiposity in male mutants was also reduced. Gonadal fat of male +/*tr* and *tr*/*tr* mice was significantly reduced compared to that of +/+ mice (Fig. 1E and F). Homozygous *Mex3c* mutant mice (*tr*/*tr*) had reduced body weights compared to those of +/+ and +/*tr* mice, regardless of age, as they were growth retarded (26). Although fat percentages of +/*tr* and *tr*/*tr* mice did not differ statistically, *tr*/*tr* mice always had smaller fat depots than +/*tr* mice (Fig. 1F). This lack of difference in fat percentage between +/*tr* and *tr*/*tr* mice was most likely caused by the significantly reduced body size of growth-retarded *tr*/*tr* mice. Indeed, other internal organs of *tr*/*tr* mice did not show a similar degree of reduction compared with +/*tr* mice (see the testes in Fig. 1F). Adipocyte sizes of +/+ and +/*tr* mice did not differ, but those of *tr*/*tr* mice were significantly reduced (Fig. 1G). Reduced adiposity in *tr*/*tr* mice was unrelated to background: in addition to the *tr*/*tr*

TABLE 3 Fecal and fecal lipid excretion of *Mex3c* mutant mice[a]

Mouse group	Fecal parameter	Mean value ± SEM for group		
		+/+	+/*tr*	*tr*/*tr*
Males	Feces (g/day)	0.91 ± 0.07	1.00 ± 0.06	0.85 ± 0.06
	Feces/food intake	0.20 ± 0.01	0.22 ± 0.01	0.21 ± 0.01
	Fecal lipid content (%)	3.6 ± 0.1	3.4 ± 0.1	3.0 ± 0.2
Females	Feces (g/day)	0.65 ± 0.09	0.75 ± 0.06	0.60 ± 0.06
	Feces/food intake	0.18 ± 0.02	0.19 ± 0.02	0.17 ± 0.01
	Fecal lipid content (%)	3.4 ± 0.2	3.5 ± 0.2	2.7 ± 0.2[b]

[a] Male mouse groups had 6 mice/genotype, and female mouse groups had 5 mice/genotype. Measurements were done at the age of 3 to 5 months. All mice were singly caged for fecal collection. Data were analyzed by Tukey's multiple-comparison test following ANOVA. *P* values of <0.05 were regarded as statistically significant.
[b] *tr*/*tr* female mice had a lower fecal lipid content than +/*tr* mice.

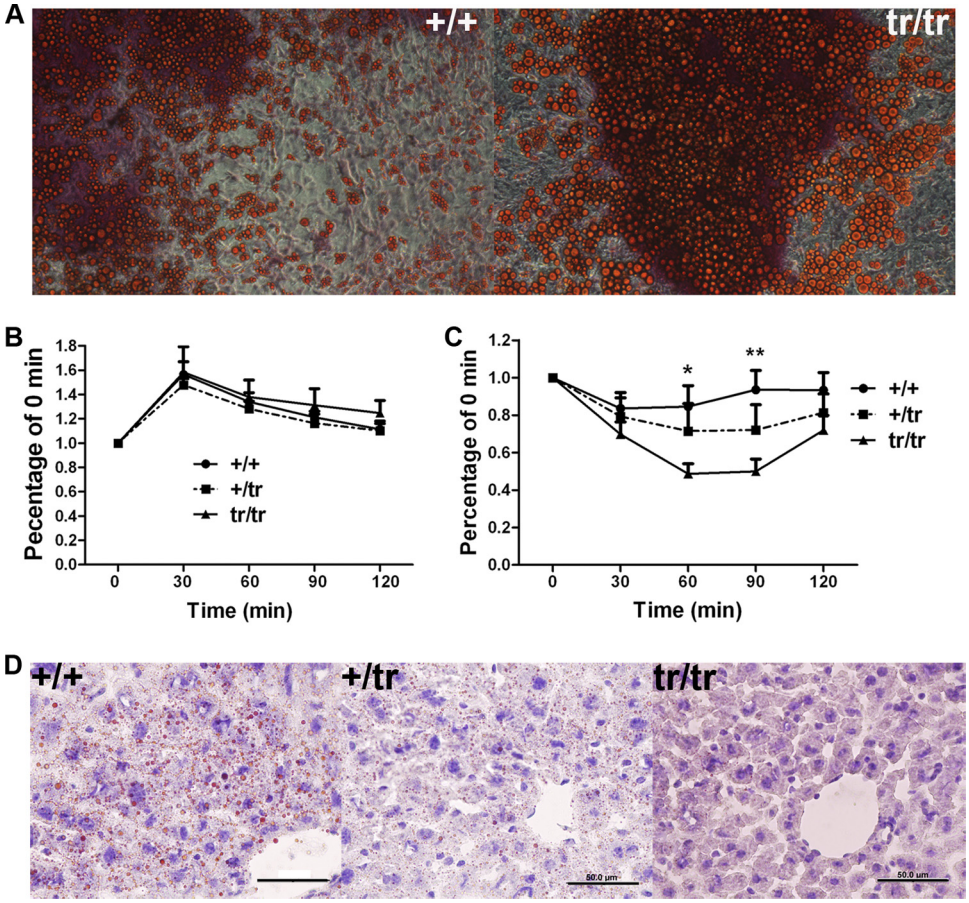

FIG 2 Normal adipogenesis and improved glucose and lipid metabolism in *Mex3c* mutant mice. (A) Similar adipocyte differentiation capacities of mouse embryonic fibroblast cells from +/+ and *tr/tr* mice. Adipocytes were stained with Oil Red O to show oil drops. (B) Normal response to glucose challenge in +/*tr* and *tr/tr* mice. (C) *tr/tr* mice showed an improved response to insulin. Blood glucose concentrations before glucose (B) or insulin (C) injection were significantly different between groups, so all values for subsequent time points were normalized to those of time zero, which were set as 1. Means ± SEM for 6 males (10 to 20 weeks old) per group are presented. * and ** indicate *P* values of <0.05 and <0.01, respectively, when *tr/tr* mice were compared with +/+ mice by Bonferroni posttests following ANOVA. (D) Reduced liver lipid storage in +/*tr* and *tr/tr* mice. Liver cryosections from 5-month-old females were stained with Oil Red O and counterstained with hematoxylin. Oil drops, which were reduced in size and number in +/*tr* mice, and especially in *tr/tr* mice, are stained red. The images shown are representative of 5 mice per group.

mice of mainly the FVB background described here, *tr/tr* mice of mainly the C57BL/6 background, a mixed C57BL/6 and 129/Sv background, and a mixed C57BL/6 and FVB/N background all had reduced adiposity. Adiposity of +/*tr* mice in these backgrounds was not examined.

***Mex3c* mutant mice have normal food intake and fecal lipid excretion.** Daily food intakes of singly caged adult +/+ and +/*tr* mice were similar (Table 2). Since +/*tr* mice showed reduced body weights compared to +/+ mice only after 5 months, we examined food intakes of mice as a function of age. Neither +/+ mice nor +/*tr* mice showed evident food intake changes during the ages of 2 to 8 months (Fig. 1H), consistent with our observations that lean masses between +/+ and +/*tr* mice were similar and that fat mass accounted for the body weight difference. These data rule out the possibility that the body weight difference between +/*tr* and +/+ mice after 5 months could be the result of changed food intake.

Young adult *tr/tr* mice quickly lost a significant amount of body weight when caged singly, possibly because they were small, had little fat, and had difficulty maintaining body temperature when singly caged. Thus, *tr/tr* mice were caged in groups (2 or 3 mice/cage) to assay food intake. Absolute daily food intake for *tr/tr* mice was significantly reduced compared to that for +/+ and +/*tr* mice (Table 2), consistent with their significantly reduced lean mass. Daily food intake normalized to body weight was not changed in *tr/tr* males but was reduced in *tr/tr* females, which may have been caused by the fact that *tr/tr* mice were caged in groups for food intake analysis, whereas the other mice were singly caged. To further test whether *tr/tr* mice had reduced food intake, they were also singly caged for food intake assay at the age of 3 months, when *tr/tr* mice were more tolerant to single caging. Food intakes normalized to lean mass were not different between +/+ and *tr/tr* mice (Table 2). The data suggested that neither +/*tr* nor *tr/tr* mice had a reduced food intake.

Fecal excretion did not differ between +/+, +/*tr*, and *tr/tr* mice (Table 3). Analysis of fecal lipid content showed comparable residual lipids in feces of +/+, +/*tr*, and *tr/tr* male mice, and female *tr/tr* mice even had reduced residual fecal lipids. The data suggested that *Mex3c* mutation did not impair lipid absorption. MEFs from 12.5-day-old control and mutant embryos were isolated for *in vitro* adipogenesis assays. MEFs from +/+ and *tr/tr*

TABLE 4 Blood glucose and lipid parameters of control and *Mex3c* mutant mice[a]

Measurement	Sex	Mean value ± SEM for group (no. of mice in group)		
		+/+	+/*tr*	*tr/tr*
Leptin (ng/ml)	Male	3.56 ± 1.07 (9)	1.90 ± 0.51 (5)	0.44 ± 0.13 (6)[c]
	Female	5.68 ± 1.68 (10)	7.81 ± 2.22 (6)	1.82 ± 0.76 (7)[c]
Glucose (mg/dl)	Male	176.0 ± 6.3 (6)	150.8 ± 9.2 (6)	113.8 ± 6.1 (6)[c,d]
	Female	175.7 ± 9.0 (5)	174.9 ± 7.8 (5)	127.6 ± 7.3 (5)[c,d]
Insulin (μg/liter)	Male	0.53 ± 0.06 (8)	1.0 ± 0.27 (5)	0.45 ± 0.06 (8)
	Female	0.82 ± 0.17 (9)	0.86 ± 0.27 (5)	0.47 ± 0.06 (8)
Triglyceride (mg/dl)	Male	124.2 ± 10.9 (9)	88.6 ± 20.1 (5)	65.5 ± 5.2 (9)[c]
	Female	147.1 ± 8.8 (10)	196.7 ± 11.2 (5)[b]	97.1 ± 9.4 (9)[c,d]
Cholesterol (mg/dl)	Male	127.4 ± 5.6 (9)	137.5 ± 18.4 (5)	*74.7 ± 6.5 (8)*[c,d]
	Female	92.4 ± 12.8 (10)	109.6 ± 3.1 (5)	61.1 ± 6.9 (9)[c,d]

[a] Mice were 5 months old. Blood glucose was measured after 16 h of fasting. Other measurements were obtained after 6 h of fasting.
[b] $P < 0.05$ for +/*tr* mice versus +/+ mice.
[c] $P < 0.05$ for *tr/tr* mice versus +/+ mice.
[d] $P < 0.05$ for *tr/tr* mice versus +/*tr* mice.

embryos both generated numerous large colonies with fully differentiated adipocytes, excluding the possibility of impaired adipogenesis in mutant mice (Fig. 2A).

MEX3C deficiency improves glucose and lipid profiles. Consistent with greatly reduced adiposity in *tr/tr* mice and the observation that blood leptin concentrations are proportional to fat mass (8), leptin levels in *tr/tr* mice were significantly lower than those in +/+ mice (Table 4). Although blood glucose levels were not significantly different between +/+ and +/*tr* mice, they were significantly reduced in *tr/tr* mice. Insulin levels did not differ among the groups. *tr/tr* mice, but not +/*tr* mice, had lower blood triglyceride and total cholesterol concentrations than those of +/+ mice (Table 4). In summary, all of the parameters assayed showed significant reductions in *tr/tr* mice compared to +/+ mice. The values for +/*tr* mice were not different from those for +/+ mice, except for +/*tr* females, which showed higher triglyceride levels than +/+ females. Due to the large intragroup variation and the relatively small group size for +/*tr* mice, the physiological significance of this difference is not clear.

+/+, +/*tr*, and *tr/tr* mice showed similar responses to intraperitoneal glucose challenge (Fig. 2B). However, *tr/tr* mice had a stronger response than that of +/+ mice in insulin tolerance assays, whereas +/*tr* mice had an intermediate response to insulin that was not significantly different from that of +/+ mice (Fig. 2C). Liver cryosections from *tr/tr* mice had fewer oil drops than those from +/+ mice (Fig. 2D). Oil drops in +/*tr* liver sections also seemed decreased, but to a lesser degree than those in *tr/tr* liver sections.

***Mex3c* mutation increases energy expenditure.** Energy expenditure was examined by indirect calorimetry for +/+ and +/*tr* mice at 12 weeks of age, when body weight and body composition were similar (Fig. 3A). The RER profile of +/*tr* mice was similar to that of +/+ mice (Fig. 3B). Locomotor activity also did not differ between +/+ and +/*tr* mice (Fig. 3C and D). However, +/*tr* mice had significantly higher oxygen consumption (Fig. 3E and F) and carbon dioxide production (Fig. 3G) than +/+ mice, during both light and dark hours. Total energy expenditure was also higher in +/*tr* mice than in +/+ mice, during both light and dark hours (Fig. 3H). *tr/tr* mice quickly lost significant weight when singly housed in metabolic cages, and thus indirect calorimetry was not performed on these mice. Although +/*tr* mice showed a higher energy expenditure, their body weight and adiposity were not different from those of +/+ mice at this age. This was most likely because adiposity was low even in +/+ mice at this age, and a difference would be detectable only at a later time, when adipose tissue constitutes a larger part of the body weight.

Analysis of fatty acid oxidation and brown fat gene expression. Fatty acid oxidation of muscle and liver, two organs involved in lipid metabolism, was compared between +/+, +/*tr*, and *tr/tr* mice, and no differences were found among the groups (Fig. 4A). Muscle glucose oxidation levels were also similar among the groups (Fig. 4B). Brown fat is involved in thermogenesis, and a comparison of *Ucp1* expression in brown fat between +/+, +/*tr*, and *tr/tr* mice did not reveal a significant difference (Fig. 4C). Consistent with the lack of difference in *Ucp1* expression, the body temperature of +/*tr* and *tr/tr* mice did not differ from that of +/+ mice (Fig. 4D), although we confirmed an earlier report that female mice have a higher body temperature than that of male mice (47). *Ucp2* was reduced 50% in +/*tr* and *tr/tr* mice, which did not explain the leanness. Expression of *Pgc-1*α, a transcription coactivator involved in mitochondrial biogenesis, was increased in brown fat of *tr/tr* mice, but not in +/*tr* mice. The expression of *Ppar*γ, a gene involved in lipid metabolism, did not differ among the three genotypes.

***Mex3c* is expressed in neurons of the central nervous system.** Following up on our recent observation of relatively high expression of *Mex3c* in the brain (26), we examined its expression in different areas of the brain by measuring β-galactosidase activity. X-Gal did not evenly stain all regions of the brain. In contrast, the strongest punctate staining was observed in cells of CA1-3 and the dentate gyrus of the hippocampus, while moderate staining was observed in the cortex and the hypothalamus (Fig. 5A). To test whether *Mex3c*-expressing cells in the brain are neurons, brain cryosections were double stained with antibodies specific to β-galactosidase (for *Mex3c*-expressing cells) and β-III tubulin (for neurons) (37). All β-galactosidase-positive cells were also positive

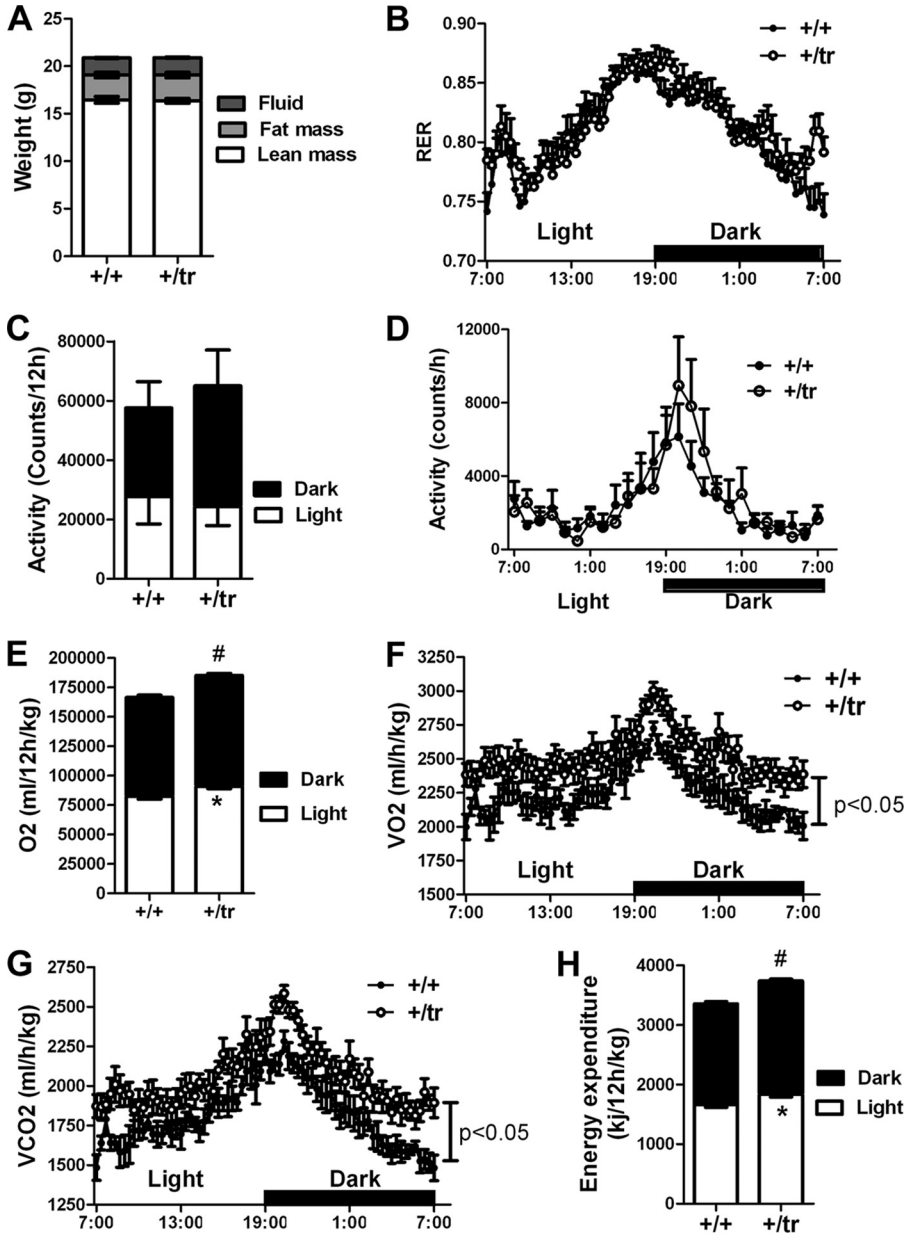

FIG 3 +/*tr* mice have increased energy expenditure. (A) Similar body weights and body compositions of mice in indirect calorimetry assay. (B) Similar RER profiles between +/+ and +/*tr* mice. (C) Similar total beam break counts between +/+ and +/*tr* mice during light and dark hours. (D) Similar physical activity profiles between +/+ and +/*tr* mice. (E) +/*tr* mice had significantly increased oxygen consumption compared to +/+ mice during light (*, $P < 0.05$) and dark (#, $P < 0.01$) hours. (F) Oxygen consumption profiles of +/+ and +/*tr* mice. (G) Carbon dioxide generation profiles of +/+ and +/*tr* mice. (H) +/*tr* mice had significantly increased energy expenditure compared to +/+ mice during light (*, $P < 0.01$) and dark (#, $P < 0.01$) hours. Means ± SEM for 6 animals/group are presented. Bonferroni posttests were performed following ANOVA. In panels B to H, the average values for 3 days for each mouse were used for comparison.

for β-III tubulin (Fig. 5B), suggesting that *Mex3c*-positive cells in the brain are neurons.

A closer examination of β-galactosidase-positive cells in the hypothalamus revealed that *Mex3c* was expressed in the ARC, VMN, and DMN (Fig. 5C). NPY/Agrp and POMC neurons in the ARC are known to be involved in energy expenditure control (2, 5, 14, 29, 36, 43, 48). The observation of *Mex3c* expression in the ARC prompted us to examine whether NPY/Agrp and POMC neurons could be involved in the leanness of +/*tr* and *tr*/*tr* mice. When we compared hypothalamic *Npy*, *Agrp*, and *Pomc* expression between +/+ and *tr*/*tr* mice, *Npy* and *Agrp* mRNAs were not significantly different between groups, but *Pomc* expression was reduced to 25% of control levels (Fig. 5D). This expression pattern could not explain leanness but is consistent with a feedback response to the observed negative energy balance in the mutants, suggesting that NPY/Agrp and POMC neurons do not play a major role in this phenotype.

To examine whether *Mex3c* is expressed in NPY/Agrp or POMC neurons in the ARC, *Npy-Gfp*; *Mex3c*$^{+/tr}$ mice and *Pomc-Gfp*; *Mex3c*$^{+/tr}$ mice were generated, in which NPY neurons and

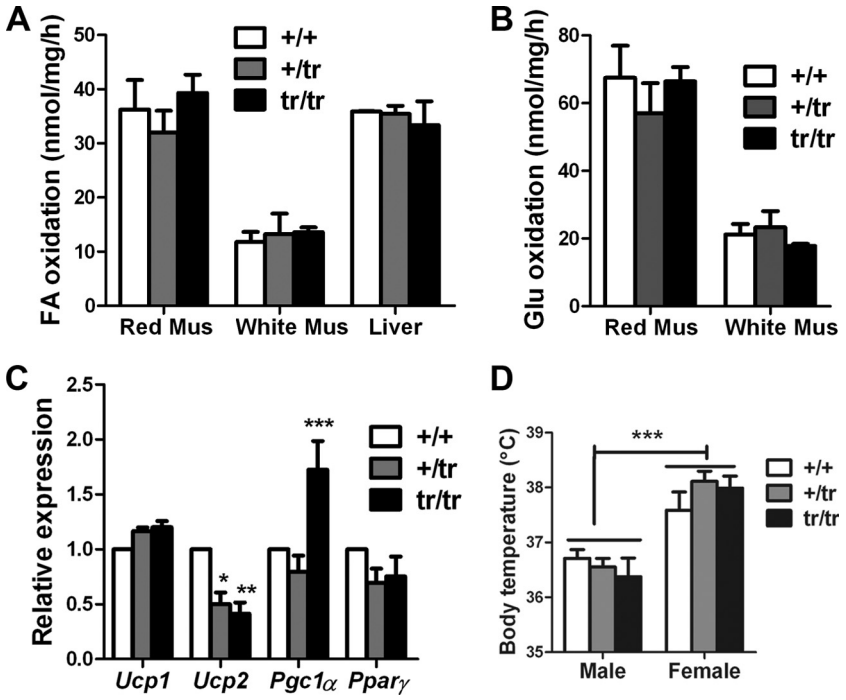

FIG 4 Analysis of peripheral tissues involved in energy balance. (A) Analysis of fatty acid (FA) oxidation in muscle and liver tissues ($n = 4$/genotype). (B) Analysis of glucose oxidation in muscle tissue ($n = 4$/genotype). (C) Analysis of gene expression in brown fat tissues by real-time RT-PCR. Equal amounts of RNA from five mice of each genotype were mixed for RT-PCR analysis. Data shown are averages for three independent PCR assays. (D) Body temperatures of +/+, +/*tr*, and *tr*/*tr* mice showed no significant difference ($n = 5$/genotype for females and $n = 6$/genotype for males). ***, $P < 0.0001$ between males and females by ANOVA. For all panels, means and SEM are shown.

POMC neurons, respectively, were labeled by GFP. In the ARC of *Npy-Gfp*; *Mex3c*$^{+/tr}$ mice, over 90% of GFP-positive cells (NPY neurons) were *Mex3c* negative (Fig. 5E). In the ARC of *Pomc-Gfp*; *Mex3c*$^{+/tr}$ mice, *Mex3c*-positive cells and GFP-positive cells (POMC neurons) were mutually exclusive (Fig. 5F). Thus, *Mex3c* has no or low expression in over 90% of NPY/Agrp neurons and 100% of POMC neurons.

To examine whether *Mex3c* is expressed in other leptin-responsive neurons, fasted +/*tr* mice were stimulated with leptin, and leptin-induced p-STAT3 was examined for colocalization with β-galactosidase (reflecting *Mex3c*-expressing cells). Leptin but not vehicle (PBS) induced STAT3 phosphorylation (Fig. 6A). In the arcuate nucleus, most p-STAT3-positive cells did not colocalize with β-galactosidase-positive cells (our unpublished data). However, in the VMH of the hypothalamus, p-STAT3 and β-galactosidase double-positive cells were readily observed (Fig. 6B), although p-STAT3-positive cells with negative galactosidase staining were also observed (arrows). All cells positive for p-STAT3 did not show nuclear localization, which could be related to the antibody and the procedure we used. Leptin-induced p-STAT3 was also not exclusively nuclear in some other studies (28, 39), including one that used the same procedure and antibody as we did. The data suggest that at least some leptin-responsive neurons express *Mex3c*.

Leptin deficiency abolishes leanness of *Mex3c* mutant mice. The expression of *Mex3c* in leptin-responsive neurons in the hypothalamus prompted us to examine the effects of leptin deficiency in *Mex3c* mutant mice, and *Mex3c* and *leptin* double mutant mice were generated. Because *Mex3c*$^{tr/tr}$ mice showed an 85% rate of perinatal lethality in the C57BL/6 background, some *Mex3c*$^{tr/tr}$; *Lep*$^{ob/ob}$ pups of a mixed C57BL/6 and FVB/N background might have been lost before weaning, since we obtained only 5 double mutant mice among 220 pups of doubly heterozygous parents, instead of the expected 14 mice. Growth of three *Mex3c*$^{tr/tr}$; *Lep*$^{ob/ob}$ mice who survived to adulthood was followed, and they were still growth retarded, with a significantly shorter stature than that of *Mex3c*$^{+/+}$; *Lep*$^{ob/ob}$ mice, at adulthood (87.0 ± 1.5 cm [$n = 3$] versus 100.3 ± 2.1 cm [$n = 4$]; $P < 0.01$). However, starting 5 weeks after birth, *Mex3c*$^{tr/tr}$; *Lep*$^{ob/ob}$ mice were heavier than *Mex3c*$^{tr/tr}$; *Lep*$^{+/+}$ mice (Fig. 7A and B), mainly because of increased fat deposition (Fig. 7C). *Mex3c*$^{+/tr}$; *Lep*$^{ob/ob}$ mice had growth curves similar to those of *Mex3c*$^{+/+}$; *Lep*$^{ob/ob}$ mice (Fig. 7A). Although *Mex3c*$^{tr/tr}$; *Lep*$^{ob/ob}$ mice had significantly less total fat mass than *Mex3c*$^{+/tr}$; *Lep*$^{ob/ob}$ and *Mex3c*$^{+/+}$; *Lep*$^{ob/ob}$ mice, the relative percentages of fat were similar among the three groups due to the shorter stature of *Mex3c*$^{tr/tr}$; *Lep*$^{ob/ob}$ mice. Thus, leptin deficiency in *Mex3c*$^{tr/tr}$; *Lep*$^{ob/ob}$ mice eliminated leanness but not growth retardation.

Blood glucose and lipid parameters were also measured for these animals. Whereas the limited sample size for each group (3 for *Mex3c*$^{+/+}$; *Lep*$^{ob/ob}$ and *Mex3c*$^{+/tr}$; *Lep*$^{ob/ob}$ mice, 2 for *Mex3c*$^{tr/tr}$; *Lep*$^{ob/ob}$ mice) may have limited our ability to detect possible differences between the three groups, blood glucose, insulin, triglyceride, and cholesterol levels were all significantly higher in mice with a mutant *Leptin* gene (Table 5) than in corresponding mice with the wild-type *Leptin* gene (Table 4), confirming the dominant effect of leptin deficiency over *Mex3c* mutation. Consistent with leptin deficiency in *Mex3c*$^{+/+}$; *Lep*$^{ob/ob}$,

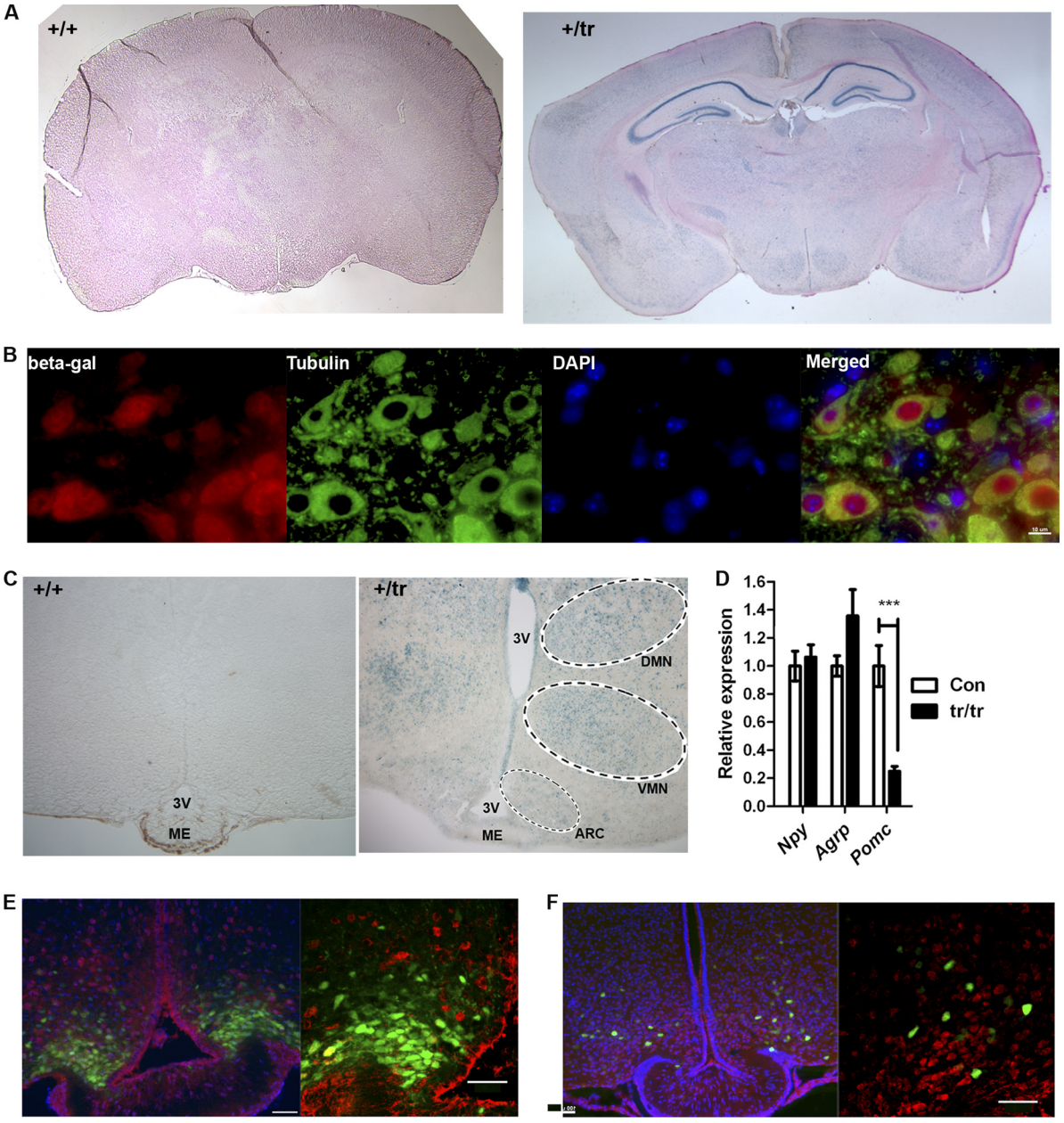

FIG 5 Expression of *Mex3c* in the brain. (A) X-Gal staining for β-galactosidase activity in brain sections from +/+ and +/*tr* mice. β-Galactosidase-positive cells stained blue (indicating *Mex3c* expression), and the section was counterstained with eosin (red). (B) β-Galactosidase-positive (*Mex3c*-expressing) cells were β-III tubulin positive. β-Galactosidase-positive cells stained red, β-III tubulin-positive cells stained green, and the nuclei stained blue (DAPI positive). (C) X-Gal staining of +/+ and +/*tr* mouse brain sections reveals the expression of *Mex3c* (blue) in the ARC, VMN, and DMN areas of the hypothalamus. 3V, third ventricle; ME, median eminence. (D) Quantitative RT-PCR analysis of *Npy*, *Agrp*, and *Pomc* expression in the hypothalami of control and *tr/tr* mice ($n = 5$ for each genotype). The peptidylprolyl isomerase B gene (*Ppib*; also called cyclophilin B) was used as an internal control. Triplicate assays were repeated at least once. ***, $P < 0.001$ by the *t* test. Means and SEM are presented. (E and F) NPY/Agrp (E) and POMC (F) neurons did not colocalize with β-galactosidase-positive cells. Brain cryosections were from *Npy-Gfp*; *Mex3c*$^{+/tr}$ (E) and *Pomc-Gfp*; *Mex3c*$^{+/tr}$ (F) mice. GFP-positive cells (green) are NPY/Agrp or POMC neurons, and red cells are β-galactosidase-positive *Mex3c*-expressing cells. (Left) Epifluorescence microscopy for a larger view. (Right) Confocal microscopy for colocalization. Blue areas are DAPI-stained nuclei. Bars, 50 μm (E), 100 μm (F, left panel), and 50 μm (F, right panel).

Mex3c$^{+/tr}$; *Lep*$^{ob/ob}$, and *Mex3c*$^{tr/tr}$; *Lep*$^{ob/ob}$ mice, leptin was undetectable in the blood of these mice. Quantitative RT-PCR was performed to examine whether *Mex3c* expression was regulated by leptin. Whereas the known leptin target gene *Socs3* was successfully induced in the hypothalamus by leptin, *Mex3c* was unaffected by leptin injection (Fig. 7D).

However, *Mex3c*$^{tr/tr}$; *Lep*$^{ob/ob}$ mice had significantly less severe liver damage than *Mex3c*$^{+/+}$; *Lep*$^{ob/ob}$ and *Mex3c*$^{+/tr}$; *Lep*$^{ob/ob}$ mice (Fig. 7E). Macrovesicular steatosis, characterized by a single large cytoplasmid lipid vacuole displacing the nucleus to the periphery of the hepatocyte, occurred in almost 100% of hepatic lobules of 5-month-old *Mex3c*$^{+/+}$; *Lep*$^{ob/ob}$ mice, whereas it was absent in age-

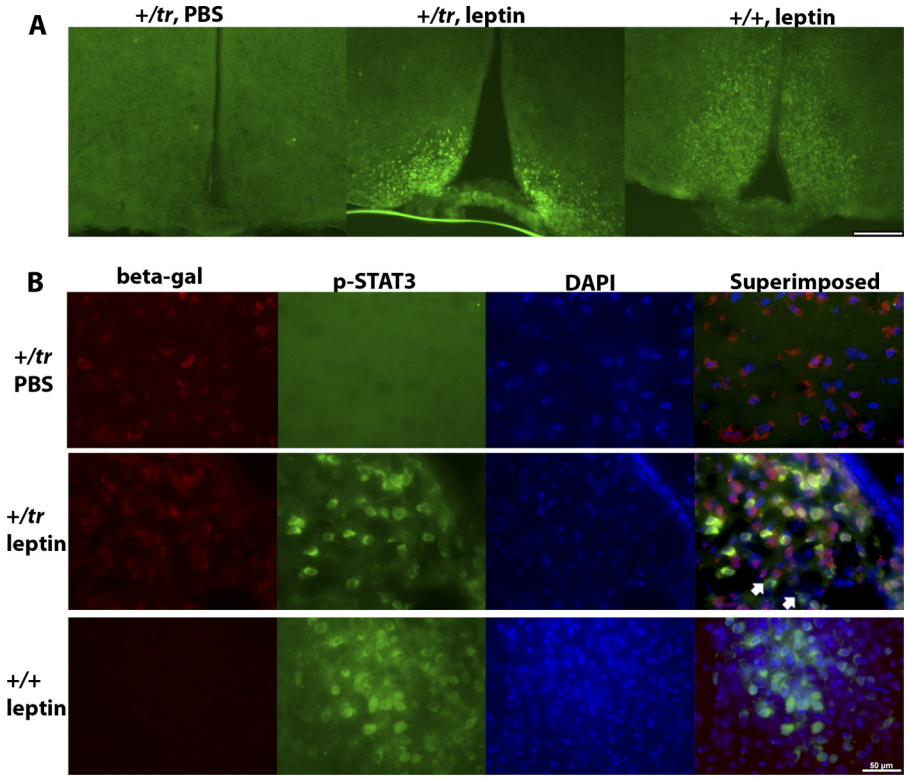

FIG 6 *Mex3c* is expressed in leptin-responsive neurons. (A) Induction of STAT3 phosphorylation by leptin. Bar, 200 μm. (B) *Mex3c* was expressed in leptin-responsive neurons. The images show p-STAT3-positive cells in the VMH of the hypothalamus. Most p-STAT3-positive cells in the field are also positive for β-galactosidase. Cells positive for p-STAT3 but negative for β-galactosidase were also observed (arrows).

matched $Mex3c^{tr/tr}$; $Lep^{ob/ob}$ mice. Hepatic damage in $Mex3c^{+/tr}$; $Lep^{ob/ob}$ mice was intermediate between that of $Mex3c^{+/+}$; $Lep^{ob/ob}$ and $Mex3c^{tr/tr}$; $Lep^{ob/ob}$ mice. Thus, hepatic damage in $Mex3c^{tr/tr}$; $Lep^{ob/ob}$ mice was qualitatively milder than that in $Mex3c^{+/+}$; $Lep^{ob/ob}$ mice, suggesting a modifying effect of *Mex3c* mutation on the phenotypes of leptin deficiency.

DISCUSSION

We observed reduced adiposity in heterozygous (+/*tr*) and homozygous (*tr/tr*) *Mex3c* gene trap mice and increased energy expenditure in +/*tr* mice. Although the energy expenditure of *tr/tr* mice was not examined due to technical issues, it may have been increased, since *tr/tr* mice were more severely affected than +/*tr* mice in many of the parameters we examined, including adiposity, adipocyte size, blood glucose levels, blood lipid levels, insulin sensitivity, and hepatic steatosis in the *ob/ob* background. These observations also suggest a dosage-dependent effect of *Mex3c* on energy balance: lower *Mex3c* expression favors a greater degree of negative energy balance.

Liver-specific inactivation of *Igf1* causes a 75 to 80% reduction of serum IGF1 and reduced fat deposition (41, 42). Although *tr/tr* mice had 40% lower serum IGF1 levels than those of wild-type mice (26), they did not have the hyperleptinemia, hyperinsulinemia, insulin insensitivity, and increased serum cholesterol observed in liver-specific *Igf1* knockout mice (41, 46). Unlike +/*tr* and *tr/tr* mice, which had increased oxygen consumption, liver-specific *Igf1* knockout mice had unchanged oxygen consumption (42). In addition, leptin deficiency in *Mex3c* mutant mice eliminated leanness but not growth retardation. Thus, IGF1 deficiency is unlikely to underlie the metabolic effects of *Mex3c* mutation. Since the *Mex3c* mutation affects both postnatal growth and adipose deposition, creating a tissue-specific *Mex3c* knockout model will be necessary to dissociate *Mex3c*'s effects on growth and metabolism.

We postulate that the leanness of +/*tr* and *tr/tr* mice is caused by increased energy expenditure but not by abnormal energy intake, as supported by the following. (i) Both +/*tr* and *tr/tr* mice had normal food intakes. Although *tr/tr* mice consumed less food each day due to growth retardation, no differences were observed after controlling for lean mass. (ii) Fecal excretion and fecal lipid content were not increased in +/*tr* or *tr/tr* mice, suggesting normal lipid absorption. (iii) Increased energy expenditure was observed in +/*tr* mice. The leanness was unlikely to have been caused by developmental defects, since (i) mouse embryonic fibroblast cells from *tr/tr* mice had a similar adipogenic capacity to that of cells from +/+ mice, suggesting that adipogenesis *per se* is not affected by *Mex3c* mutation; (ii) +/*tr* mice did not show growth retardation but had reduced adiposity at 5 months of age; (iii) other internal organs, such as the heart, the liver, and the lungs, were not reduced to the same degree in *tr/tr* mice; and (iv) leptin deficiency in *tr/tr* mice eliminated leanness but not growth retardation, suggesting that growth retardation and reduced adiposity were not intimately related in *Mex3c* mutant mice.

Our data suggest that *Mex3c* mutation might have affected central nervous system regulation of energy expenditure in +/*tr* and *tr/tr* mice. This notion is supported by our observations of *Mex3c*'s

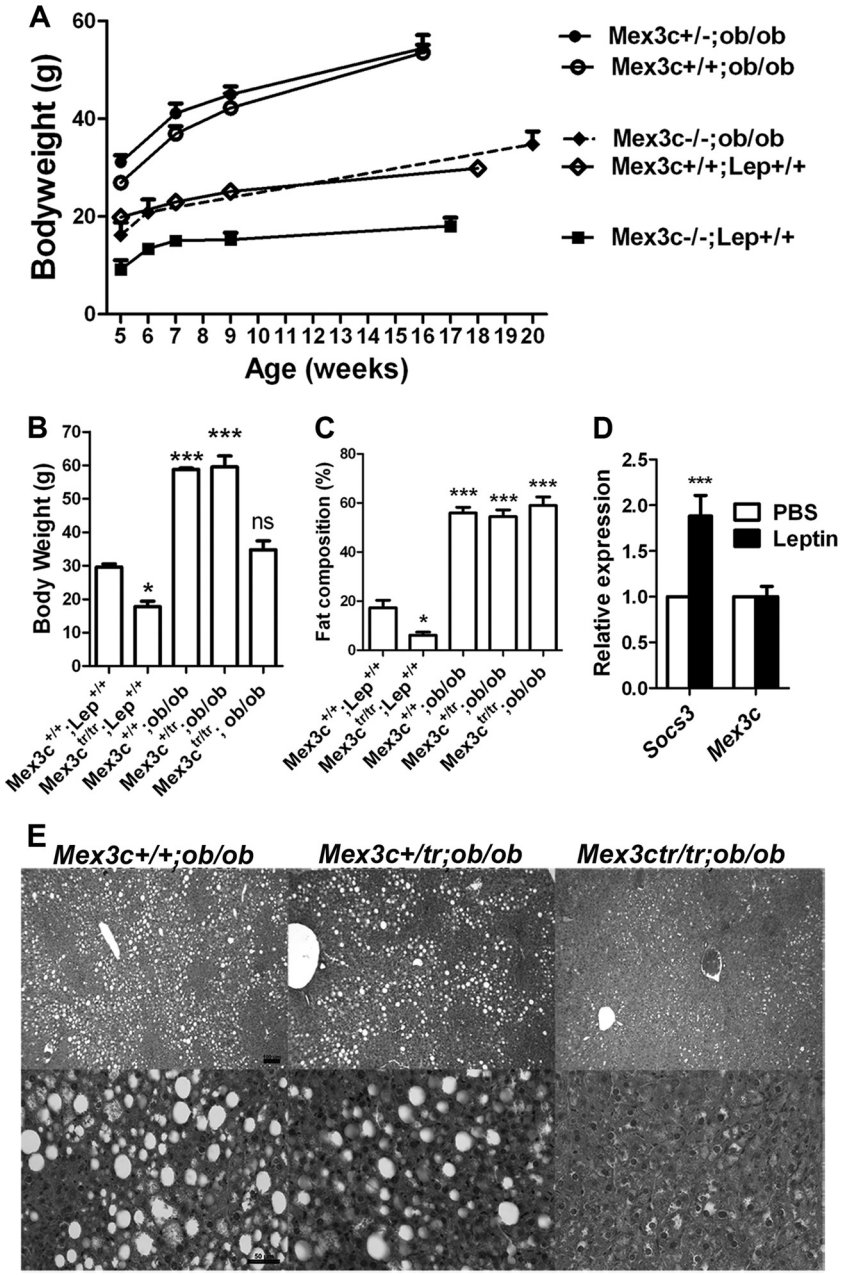

FIG 7 Obesity but no steatosis in *Mex3c*$^{tr/tr}$; *ob/ob* mice. (A) Growth curves for *Mex3c* and *Leptin* double mutant mice ($n = 3$ for *Mex3c*$^{tr/tr}$; *ob/ob* mice and $n \geq 5$ for the rest of the groups). Data are for male and female mice. No difference was observed between *Mex3c*$^{tr/+}$; *ob/ob* and *Mex3c*$^{+/+}$; *ob/ob* mice (ANOVA). (B and C) Body weights (B) and fat compositions (C) of 5-month-old mice. * and *** indicate *P* values of <0.05 and <0.0001, respectively, compared with *Mex3c*$^{+/+}$; *Lep*$^{+/+}$ mice by Tukey posttests following ANOVA ($n \geq 3$ for each group). (D) *Mex3c* expression in the mouse hypothalamus was not affected by leptin. Four mice were injected with PBS or leptin (5 μg/g body weight), and 2 h later, they were sacrificed to purify total RNA from the hypothalamus. Equal RNA from each mouse receiving the same injection was mixed for quantitative RT-PCR analysis. ***, $P < 0.0001$ by two-way ANOVA. (E) No liver steatosis in *Mex3c*$^{tr/tr}$; *ob/ob* mice. The images show representative pictures for three mice examined per group. (Top) Low-magnification view; (bottom) high-magnification view. In panels A to D, means ± SEM are shown.

low expression in peripheral tissues involved in lipid metabolism yet high expression in neurons of the brain (26), especially in the hypothalamic ARC, VMN and DMN, with important roles in energy homeostasis regulation (10, 11, 15). In addition, we observed normal fatty acid oxidation in liver and muscle tissues from mutant mice. *Pgc-1α* expression in brown adipose tissue is not increased in +/*tr* mice, although it is increased in *tr/tr* mice, and this increase could not explain the leanness, since whole-body *Pgc-1α* transgenic mice do not show changes in body weight or fat composition (30). It could be a feedback response to the *tr/tr* mouse's inefficiency in maintaining body temperature due to small size and reduced fat. Similarly, the reduction in *Ucp2* expression in +/*tr* and *tr/tr* mice could be a response to their negative energy balance, since the main function for *Ucp2* is to reduce the gener-

TABLE 5 Blood analysis of *Mex3c* and *Leptin* double mutant mice[a]

Measurement	Mean value ± SEM for group[b]:		
	Mex3c$^{+/+}$; *Lep*$^{ob/ob}$	*Mex3c*$^{+/tr}$; *Lep*$^{ob/ob}$	*Mex3c*$^{tr/tr}$; *Lep*$^{ob/ob}$
Glucose (mg/dl)	299.3 ± 50.8	235.3 ± 39.9	227.0 (225, 229)
Insulin (μg/liter)	68.6 ± 19.2	43.7 ± 14.5	51.7 (82.0, 21.3)
Triglyceride (mg/dl)	272.3 ± 48.2	218.8 ± 73.0	259.9 (213.3, 306.5)
Cholesterol (mg/dl)	146.0 ± 17.1	175.9 ± 16.1	142.5 (155.1, 129.9)

[a] Samples were collected after 6 h of fasting. The *Mex3c*$^{+/+}$; *Lep*$^{ob/ob}$ and *Mex3c*$^{+/tr}$; *Lep*$^{ob/ob}$ groups each had three animals, and the *Mex3c*$^{tr/tr}$; *Lep*$^{ob/ob}$ group had two. Except for one *Mex3c*$^{tr/tr}$; *Lep*$^{ob/ob}$ mouse which was female, the rest of the mice were males. Statistical comparison between the three groups was not attempted due to the small sample size.

[b] Except for *Mex3c*$^{tr/tr}$; *Lep*$^{ob/ob}$ mice, for which the values for the two mice are listed after the means.

ation of reactive oxygen species by uncoupling the overflow of NADH and $FADH_2$ from glucose and lipid oxidation (33). The observations that *Mex3c* mutant mice had a normal body temperature and that brown adipose tissue had relatively low *Mex3c* expression (our unpublished data) also argue against a major role of brown adipose tissue in the leanness of *Mex3c* mutant mice. Although energy expenditure is increased in *Mex3c* mutant mice, other mechanisms may also contribute to the leanness of *Mex3c* mutant mice. For example, central nervous system leptin has lipolytic actions on adipocyte metabolism when the autonomic innervation of fat tissue is intact (4).

Data from double mutant mice showed that leptin deficiency completely abolished the metabolic effects of *Mex3c* mutation, although *Mex3c* had a modifying effect on the phenotype of leptin deficiency. Several possibilities can explain these observations. (i) MEX3C, an RNA-binding protein, could regulate mRNAs encoding proteins modulating leptin signaling. Many proteins, such as SOCS3, PTP1B, SH2B, and SHP1, can regulate leptin signaling. If MEX3C regulates known and unknown molecules involved in leptin signaling, then the leanness of *Mex3c* mutants is expected to be eliminated in the absence of leptin. The expression of *Mex3c* in the ARC, VMN, and DMN of the hypothalamus, which are positive for leptin receptors (15), especially in leptin-responsive neurons, provides the anatomical basis for this possibility. Although *Leptin* and *Mex3c* double mutant mice were obese, they had milder liver damage than that of mice with only *Leptin* mutation. This suggests that *Mex3c* also functions independent of leptin signaling. Thus, if MEX3C regulates leptin signaling, it must also regulate additional molecules outside the leptin signaling pathway. (ii) MEX3C does not regulate leptin signaling but regulates other signaling pathways involved in energy balance, such as insulin signaling, and the leanness effects of *Mex3c* mutation could be overridden by the lack of leptin signaling. Whatever mechanisms are responsible, it is possible that *Mex3c* is involved in central regulation of energy balance.

Most NPY/Agrp and POMC neurons in the ARC expressed undetectable *Mex3c*, and the expression pattern of *Npy*, *Agrp*, and *Pomc* in *tr/tr* mice could not explain the observed leanness. Instead, the data suggest a normal feedback response to reduced adiposity, meaning that NPY/Agrp and POMC neurons in the ARC are unlikely to be involved in the leanness of *Mex3c* mutant mice. Other *Mex3c*-positive neuron types in the ARC, VMN, and DMN could have been affected by the mutation. Damage to SF-1-positive neurons in the VMN causes obesity, mainly through abnormal energy expenditure rather than increased food intake (11, 34). It is unknown whether the SF-1-positive neurons are also *Mex3c* positive; this possibility exists, since *Mex3c* is expressed in leptin-responsive neurons, where the SF-1-positive neurons are found.

Several important issues are raised by this study and need to be addressed in future research. First, if the central nervous system is involved in the leanness of *Mex3c* mutant mice, what are the identities of the *Mex3c*-positive neurons involved in the process? The evident effects of *Mex3c* mutation on energy balance (leanness even in heterozygous mice) highlight the important roles of these neurons in this process. Although the identity of *Mex3c*-positive neurons remains unknown, MEX3C could be a useful marker to define new groups of neurons in the brain which may play important roles in energy homeostasis. Second, what are the target mRNA molecules regulated by MEX3C and involved in energy balance? Identification of MEX3C-regulated mRNAs will greatly improve our understanding of how energy balance is regulated at the molecular level.

Without inhibiting food intake, *Mex3c* mutation produced multiple beneficiary effects on glucose and lipid metabolism. Mutant mice had lower blood glucose and blood lipid concentrations and increased insulin sensitivity. In addition, *Mex3c* mutation ameliorated the hepatic steatosis seen with leptin deficiency. These effects of *Mex3c* mutation might explain why the human *MEX3C* locus is associated with hypertension (21). Although *Mex3c* mutation causes growth retardation during development, MEX3C and its targets could be promising drug targets for controlling age-associated obesity and obesity-associated metabolic syndromes.

ACKNOWLEDGMENTS

We thank Yu Zhou at Wake Forest University Health Sciences for her help on cell isolation and differentiation, Karen Klein (Research Support Core, Office of Research, Wake Forest University Health Sciences) for editing the manuscript, and Haiyan Zhang and Ryan McMillan at Virginia Tech for help with fatty acid oxidation, fat composition, and metabolic analysis.

REFERENCES

1. **Agoulnik AI, et al.** 2002. A novel gene, Pog, is necessary for primordial germ cell proliferation in the mouse and underlies the germ cell deficient mutation, gcd. Hum. Mol. Genet. **11**:3047–3053.
2. **Broberger C, Johansen J, Johansson C, Schalling M, Hokfelt T.** 1998. The neuropeptide Y/agouti gene-related protein (AGRP) brain circuitry in normal, anorectic, and monosodium glutamate-treated mice. Proc. Natl. Acad. Sci. U. S. A. **95**:15043–15048.
3. **Buchet-Poyau K, et al.** 2007. Identification and characterization of human Mex-3 proteins, a novel family of evolutionarily conserved RNA-binding proteins differentially localized to processing bodies. Nucleic Acids Res. **35**:1289–1300.
4. **Buettner C, et al.** 2008. Leptin controls adipose tissue lipogenesis via central, STAT3-independent mechanisms. Nat. Med. **14**:667–675.
5. **Bultman SJ, Michaud EJ, Woychik RP.** 1992. Molecular characterization of the mouse agouti locus. Cell **71**:1195–1204.
6. **Ciosk R, DePalma M, Priess JR.** 2004. ATX-2, the C. elegans ortholog of ataxin 2, functions in translational regulation in the germline. Development **131**:4831–4841.
7. **Ciosk R, DePalma M, Priess JR.** 2006. Translational regulators maintain totipotency in the Caenorhabditis elegans germline. Science **311**:851–853.
8. **Considine RV, et al.** 1996. Serum immunoreactive-leptin concentrations in normal-weight and obese humans. N. Engl. J. Med. **334**:292–295.
9. **Courchet J, et al.** 2008. Interaction with 14-3-3 adaptors regulates the sorting of hMex-3B RNA-binding protein to distinct classes of RNA granules. J. Biol. Chem. **283**:32131–32142.

10. **Cowley MA, et al.** 2001. Leptin activates anorexigenic POMC neurons through a neural network in the arcuate nucleus. Nature **411**:480–484.
11. **Dhillon H, et al.** 2006. Leptin directly activates SF1 neurons in the VMH, and this action by leptin is required for normal body-weight homeostasis. Neuron **49**:191–203.
12. **Donnini M, et al.** 2004. Identification of TINO: a new evolutionarily conserved BCL-2 AU-rich element RNA-binding protein. J. Biol. Chem. **279**:20154–20166.
13. **Draper BW, Mello CC, Bowerman B, Hardin J, Priess JR.** 1996. MEX-3 is a KH domain protein that regulates blastomere identity in early C. elegans embryos. Cell **87**:205–216.
14. **Fan W, Boston BA, Kesterson RA, Hruby VJ, Cone RD.** 1997. Role of melanocortinergic neurons in feeding and the agouti obesity syndrome. Nature **385**:165–168.
15. **Fei H, et al.** 1997. Anatomic localization of alternatively spliced leptin receptors (Ob-R) in mouse brain and other tissues. Proc. Natl. Acad. Sci. U. S. A. **94**:7001–7005.
16. **Folch J, Lees M, Sloane Stanley GH.** 1957. A simple method for the isolation and purification of total lipids from animal tissues. J. Biol. Chem. **226**:497–509.
17. **Frisard MI, et al.** 2010. Toll-like receptor 4 modulates skeletal muscle substrate metabolism. Am. J. Physiol. Endocrinol. Metab. **298**:E988–E998.
18. **Gantz I, et al.** 1993. Molecular cloning, expression, and gene localization of a fourth melanocortin receptor. J. Biol. Chem. **268**:15174–15179.
19. **George SK, Jiao Y, Bishop CE, Lu B.** 2011. Mitochondrial peptidase IMMP2L mutation causes early onset of age-associated disorders and impairs adult stem cell self-renewal. Aging Cell **10**:584–594.
20. **George SK, Jiao Y, Bishop CE, Lu B.** 2012. Oxidative stress is involved in age-dependent spermatogenic damage of Immp2l mutant mice. Free Radic. Biol. Med. **52**:2223–2233.
21. **Guzman B, et al.** 2006. Implication of chromosome 18 in hypertension by sibling pair and association analyses: putative involvement of the RKHD2 gene. Hypertension **48**:883–891.
22. **Huang NN, Mootz DE, Walhout AJM, Vidal M, Hunter CP.** 2002. MEX-3 interacting proteins link cell polarity to asymmetric gene expression in Caenorhabditis elegans. Development **129**:747–759.
23. **Hunter CP, Kenyon C.** 1996. Spatial and temporal controls target pal-1 blastomere-specification activity to a single blastomere lineage in C. elegans embryos. Cell **87**:217–226.
24. **Huszar D, et al.** 1997. Targeted disruption of the melanocortin-4 receptor results in obesity in mice. Cell **88**:131–141.
25. **Jadhav S, Rana M, Subramaniam K.** 2008. Multiple maternal proteins coordinate to restrict the translation of C. elegans nanos-2 to primordial germ cells. Development **135**:1803–1812.
26. **Jiao Y, Bishop CE, Lu B.** 2012. Mex3c regulates insulin-like growth factor 1 (IGF1) expression and promotes postnatal growth. Mol. Biol. Cell **23**:1404–1413.
27. **Johnson DH, Flask CA, Ernsberger PR, Wong WC, Wilson DL.** 2008. Reproducible MRI measurement of adipose tissue volumes in genetic and dietary rodent obesity models. J. Magn. Reson. Imaging **28**:915–927.
28. **Kim KS, et al.** 2010. Enhanced hypothalamic leptin signaling in mice lacking dopamine D2 receptors. J. Biol. Chem. **285**:8905–8917.
29. **Kristensen P, et al.** 1998. Hypothalamic CART is a new anorectic peptide regulated by leptin. Nature **393**:72–76.
30. **Liang H, et al.** 2009. Whole body overexpression of PGC-1alpha has opposite effects on hepatic and muscle insulin sensitivity. Am. J. Physiol. Endocrinol. Metab. **296**:E945–E954.
31. **Lillie RD, Ashburn LL.** 1943. Supersaturated solutions of fat stains in dilute isopropanol for demonstration of acute fatty degeneration not shown by Herxheimer's technique. Arch. Pathol. **36**:432.
32. **Lu D, et al.** 1994. Agouti protein is an antagonist of the melanocyte-stimulating-hormone receptor. Nature **371**:799–802.
33. **Mailloux RJ, Harper ME.** 2011. Uncoupling proteins and the control of mitochondrial reactive oxygen species production. Free Radic. Biol. Med. **51**:1106–1115.
34. **Majdic G, et al.** 2002. Knockout mice lacking steroidogenic factor 1 are a novel genetic model of hypothalamic obesity. Endocrinology **143**:607–614.
35. **Mayer J, Thomas DW.** 1967. Regulation of food intake and obesity. Science **156**:328–337.
36. **Miller MW, et al.** 1993. Cloning of the mouse agouti gene predicts a secreted protein ubiquitously expressed in mice carrying the lethal yellow mutation. Genes Dev. **7**:454–467.
37. **Moody SA, Quigg MS, Frankfurter A.** 1989. Development of the peripheral trigeminal system in the chick revealed by an isotype-specific anti-beta-tubulin monoclonal antibody. J. Comp. Neurol. **279**:567–580.
38. **Mountjoy KG, Mortrud MT, Low MJ, Simerly RB, Cone RD.** 1994. Localization of the melanocortin-4 receptor (MC4-R) in neuroendocrine and autonomic control circuits in the brain. Mol. Endocrinol. **8**:1298–1308.
39. **Munzberg H, Huo L, Nillni EA, Hollenberg AN, Bjorbaek C.** 2003. Role of signal transducer and activator of transcription 3 in regulation of hypothalamic proopiomelanocortin gene expression by leptin. Endocrinology **144**:2121–2131.
40. **Musco G, et al.** 1996. Three-dimensional structure and stability of the KH domain: molecular insights into the fragile X syndrome. Cell **85**:237–2451.
40a. **National Research Council.** 1996. Guide for the care and use of laboratory animals. National Academies Press, Washington, DC.
41. **Sjogren K, et al.** 2001. Liver-derived IGF-I is of importance for normal carbohydrate and lipid metabolism. Diabetes **50**:1539–1545.
42. **Svensson J, et al.** 2011. Liver-derived IGF-I regulates mean life span in mice. PLoS One **6**:e22640. doi:10.1371/journal.pone.0022640.
43. **Tsujii S, Bray GA.** 1989. Acetylation alters the feeding response to MSH and beta-endorphin. Brain Res. Bull. **23**:165–169.
44. **van den Pol AN, et al.** 2009. Neuromedin B and gastrin-releasing peptide excite arcuate nucleus neuropeptide Y neurons in a novel transgenic mouse expressing strong Renilla green fluorescent protein in NPY neurons. J. Neurosci. **29**:4622–4639.
45. **Weir JB.** 1949. New methods for calculating metabolic rate with special reference to protein metabolism. J. Physiol. **109**:1–9.
46. **Yakar S, et al.** 2001. Liver-specific igf-1 gene deletion leads to muscle insulin insensitivity. Diabetes **50**:1110–1118.
47. **Yang JN, Chen JF, Fredholm BB.** 2009. Physiological roles of A1 and A2A adenosine receptors in regulating heart rate, body temperature, and locomotion as revealed using knockout mice and caffeine. Am. J. Physiol. Heart Circ. Physiol. **296**:H1141–H1149.
48. **Zarjevski N, Cusin I, Vettor R, Rohner-Jeanrenaud F, Jeanrenaud B.** 1993. Chronic intracerebroventricular neuropeptide-Y administration to normal rats mimics hormonal and metabolic changes of obesity. Endocrinology **133**:1753–1758.
49. **Zhang Y, et al.** 1994. Positional cloning of the mouse obese gene and its human homologue. Nature **372**:425–432.